

Report at the 7-th Russian-Japanese international simposium on computational fluid dynamics. Moscow, July 31 - August 6, 2000.

FLOWS OF CONDENSED MATERIALS WITH MOVING BOUNDARIES

A.A.Charakhch'yan

Computing Center of the Russian Academy of Sciences,

Russia 117967, Moscow GSP-1, ul. Vavilova 40

E-mail: chara@ccas.ru

This paper reviews of recent works by the author dealing with shock-induced time-dependent flows of condensed materials and accompanying problems of computational fluid dynamics. A new regular barrier-type grid generator [1] is considered in Section 1. Section 2 deals with suppressing false entropy wakes which can arise in interaction of finite-difference shock waves with boundaries [2]. The instability of a free aluminum surface due to passage of two successive shocks [3] and shock compression of graphite in conic targets with channels [4] are considered in Sections 3 and 4 respectively.

1. Elliptic Grid Generator Based on Quasi-1D Grids

A problem of constructing 2D regular grids is considered in the following standard formulation. The grid $G = \{\vec{r}_{ij}, i = 0, \dots, N; j = 0, \dots, M\}$, $\vec{r}_{ij} = (x, y)_{ij}$ should be constructed while the boundary grid nodes $\vec{r}_{i0}, \vec{r}_{iM}, \vec{r}_{0j}, \vec{r}_{Nj}$ are given. The method [5] is based on minimization of a function $I(G)$ with the following barrier property. Let D be the set of convex grids (consisting of only convex quadrilateral cells), ∂D be its boundary. If $G \rightarrow \partial D$ for $G \in D$, then $I^h(G) \rightarrow +\infty$. As a result, $G_n \in D$ at each iteration step n , which prevents from self-intersecting cells for any boundary grid lines.

Nevertheless, the method [5] has the drawback which is illustrated by Fig.1. The grid does not enter the tongues at the down part of the domain. As a result, the grid cells in the tongues are too large.

Our new grid generator uses positive properties of quasi-1D grids for which the grid lines of one of two families are straight lines with a given allocation law of grid points along the lines. We construct the function $Q(G)$ which reaches its minimum at the quasi-1D grid and consider the function $J(G) = Q(G) + \varepsilon\sigma I(G)$ where ε is a small parameter, σ is the average area of a grid cell introduced to obtain a dimensionless parameter ε . Since this function has the same barrier property as the function $I(G)$ for any $\varepsilon > 0$, the grid generator based on minimization of $J(G)$ is also very reliable. Fig. 2 shows that the method yields a much more dense grid inside the tongues, with all grid cells being convex.

2. Suppressing false entropy wakes

The idea of such suppressing is as follows. Consider the Godunov scheme in lagrangian variables for a certain grid cell i, j . When solving the Riemann problems at the cell boundaries, we can determine the maximal entropy S_{\max} among the shock waves going within the cell. Let S^{ij} be the entropy in the cell at the upper time level given by the scheme. If $S^{ij} < S_{\max}$, the values at the upper time level are unchanged. If $S^{ij} > S_{\max}$, the thermodynamic functions at the upper time level in the cell are corrected by the following way. One of the functions, for example the pressure p , is unchanged while the others are determined on the isentrope corresponding S_{\max} .

Realization of this idea is some more complex. First, the entropies of the neighboring cells at the lower time level $S_{i+l, j+k}$, $j, k = -1, 0, 1$ are also taken into account in computing S_{\max} . Second, instead of the entropy S , it is more convenient to use the entropy temperature $T_S = T(S, \rho_*)$ for a certain fixed density ρ_* . The function $T_S = T_S(T, \rho)$ is determined by computing the isentrope from the point (T, ρ) to ρ_* . In determining $(T_S)_{\max}$ and $(T_S)^{ij}$ in the cell i, j we put $\rho_* = \rho_{ij}$.

In Fig. 3 we illustrate the method with two 1D problems: impact of an aluminum plate with the velocity 5 km/s on the rigid wall and interaction of the shock wave (1 Mbar) in aluminum and a free boundary. Here the entropy temperature T_S is determined for ρ_* being equal to normal aluminum density. It is shown that our method suppresses the entropy wakes.

In Fig. 4 we use the 2D problem on compression of an aluminum plate on a lead wedge by a shock wave to illustrate the method. A second order accurate quasi-monotone scheme with splitting on lagrangian and remapping stages is used and is called below as the routine scheme. For a variant presented in Fig. 4 a cumulative jet arises. It is shown that the routine scheme gives an entropy wake near the free boundary of aluminum which penetrates into the cumulative jet. The corrected scheme suppresses the wake.

3. Richtmyer-Meshkov Instability. Reshocking at Non-Linear Stage

The instability of an interface between two media with different densities ρ_1 and ρ_2 due to passage of two successive shocks is considered in the case of Atwood number $A = (\rho_2 - \rho_1)/(\rho_2 + \rho_1) < 0$. Let a be the perturbation amplitude at the moment when the second shock reaches the interface and λ be the wavelength. If the relative amplitude $\beta = 2\pi a/\lambda \ll 1$, the reshocking is described by the Richtmyer formula: $\Delta\dot{a} = \dot{a}_2 - \dot{a}_1 = \beta A \Delta v$, where \dot{a}_1 and \dot{a}_2 are the amplitude growth rate before and after passage of the second shock, Δv is the change of the interface velocity. The well known freeze-out effect [6] is that such value of $\Delta v > 0$ exists for which $\dot{a}_2 = 0$. The effect has no practical utilization since Δv depends on λ .

We check the hypothesis that the reshocking at non-linear stage ($\beta \sim 1$) is approximately described by the formula

$$\Delta\dot{a} = \beta^* A \Delta v, \quad \beta^* = \text{const} = 1, 25 \quad (1)$$

which is independent of λ . For this purpose we consider the instability of a free boundary ($A = -1$) of an aluminum layer. At the opposite boundary of the layer a boundary condition initiating two successive shocks is considered. For freeze-out effect ($\dot{a}_2 = 0$) (1) gives $\Delta v = -\dot{a}_1/A\beta^*$ where \dot{a}_1 is determined from a 2D computation without a second shock. A set of 1D computations allows to determine parameters of the boundary condition as a function of Δv . The results of the corresponding reshocking are presented in Fig. 5 both for sinusoidal and for non-sinusoidal (broken line with three segments) initial perturbations. One can see that the freeze-out effect takes place in the all cases.

4. Shock Compression of Graphite in Conic Targets

Graphite compression in lead conic targets with aluminum strikers is simulated numerically. A model of non-equilibrium phase transition of graphite to diamond is taken into account. Both the routine conic target and the target with a channel (Fig. 6) are considered.

Fig. 6 presents one of computed variants. An interesting feature of the flow is connected with the unloading of carbon after shock compression which turns out to be very similar to 1D unloading of lead and very far from 1D unloading of carbon.

Acknowledgments

Modeling of graphite compression from Section 4 is performed jointly with K.V.Khishchenko, I.V.Lomonosov, V.E.Fortov, A.A.Frolova and L.V.Shurshalov. The author is also grateful to K.V.Khishchenko and I.V.Lomonosov for tables of equations of state.

This work is supported by the Russian Foundation for Basic Research (Project No. 00-01-00551).

References

1. Charakhch'yan A.A., *Comput. Maths. Math. Phys.*, **39**, No. 5, 799 (1999).
2. Charakhch'yan A.A., *Comput. Maths. Math. Phys.*, **40**, No. 5, 746 (2000).
3. Charakhch'yan A.A., *J. Appl. Mechan. Technical Phys.*, **41**, No. 1, 23 (2000).
4. Lomonosov I.V., Fortov V.E., Frolova A.A., Khishchenko K.V., Charakhch'yan A.A., Shurshalov L.V., *Doklady Phycics*, **43**, No. 5, 306-308 (1998).
5. Ivanenko S.A., Charakhch'yan A.A., *Soviet. Math. Dokl.*, **36**, No. 1, 51 (1988); *USSR Comput. Maths Math. Phys* **28**, No. 2, 126 (1988); *J. Comput. Phys.* **136**, No. 2, 385 (1997).
6. Mikaelian K.O., *Phys. Rev. A*, **31**, No. 1, 410 (1985).

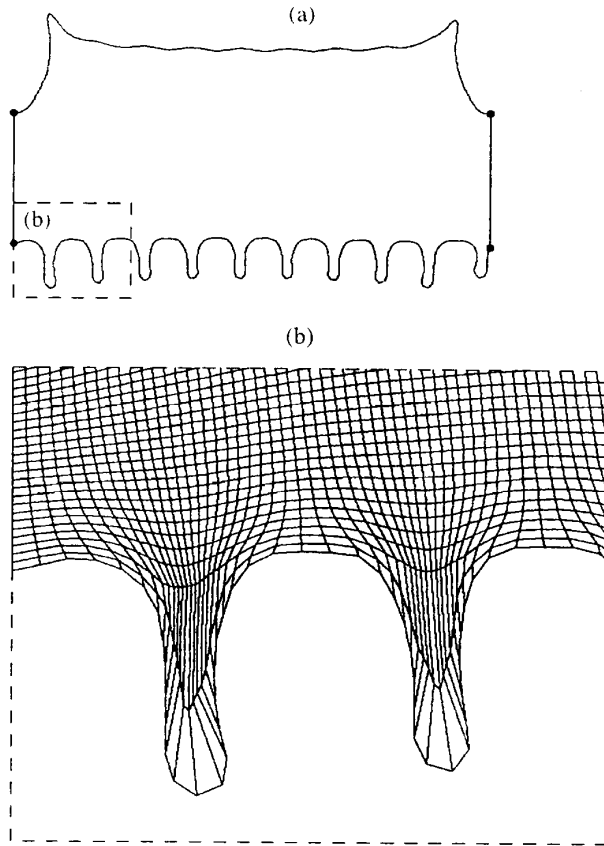


Figure 1: A domain and a fragment of the grid for the method [5].

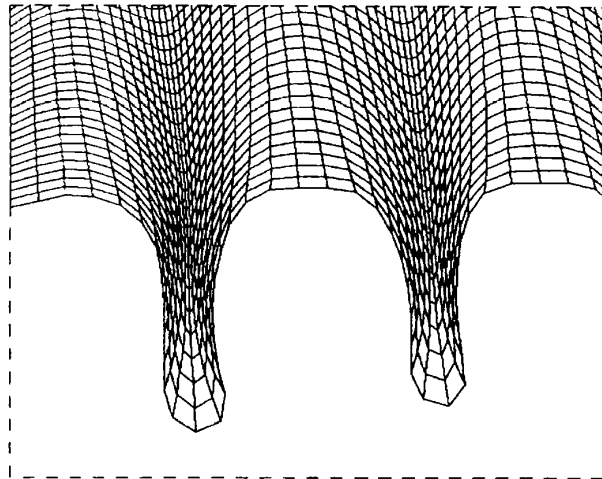


Figure 2: The suggested method, $\varepsilon = 10^{-2}$.

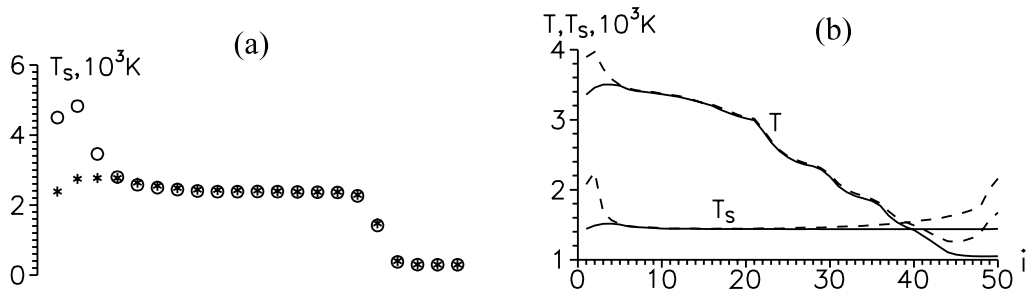


Figure 3: (a) Impact on the rigid wall (left side) using the routine scheme (circles) and the corrected scheme (stars). (b) Interaction of a shock wave and a free boundary (right side) using the routine scheme (dashed line) and the corrected scheme (solid line); i is the cell number.

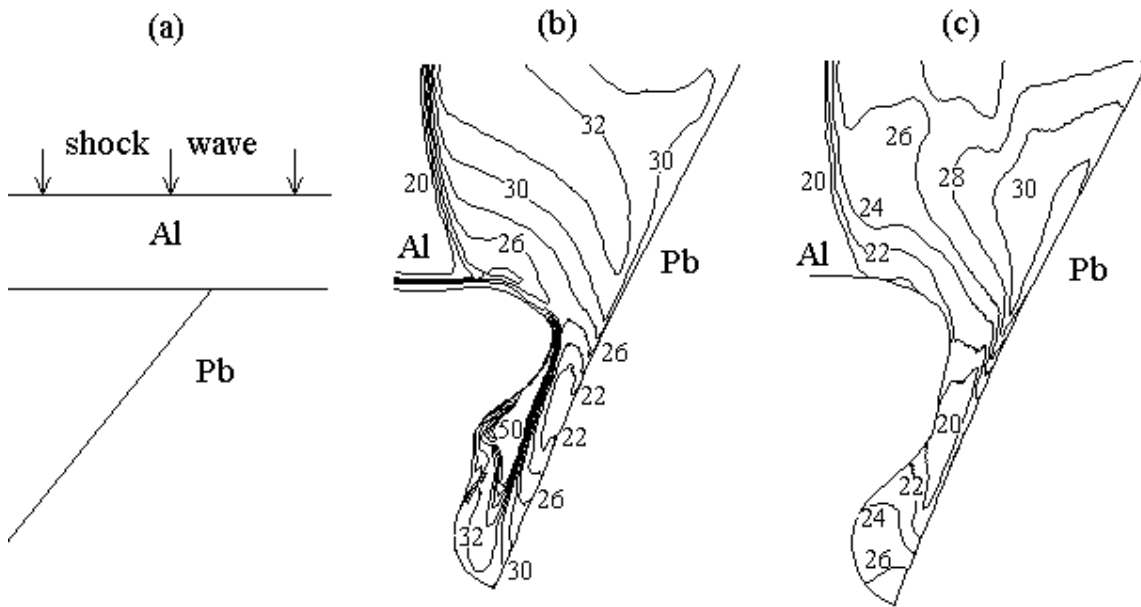


Figure 4: Compression of a plate on a wedge; (a) the scheme of the problem; (b) isotherms (10^2 K) in the vicinity of the cumulative jet for the routine scheme; (c) the same for the corrected scheme.

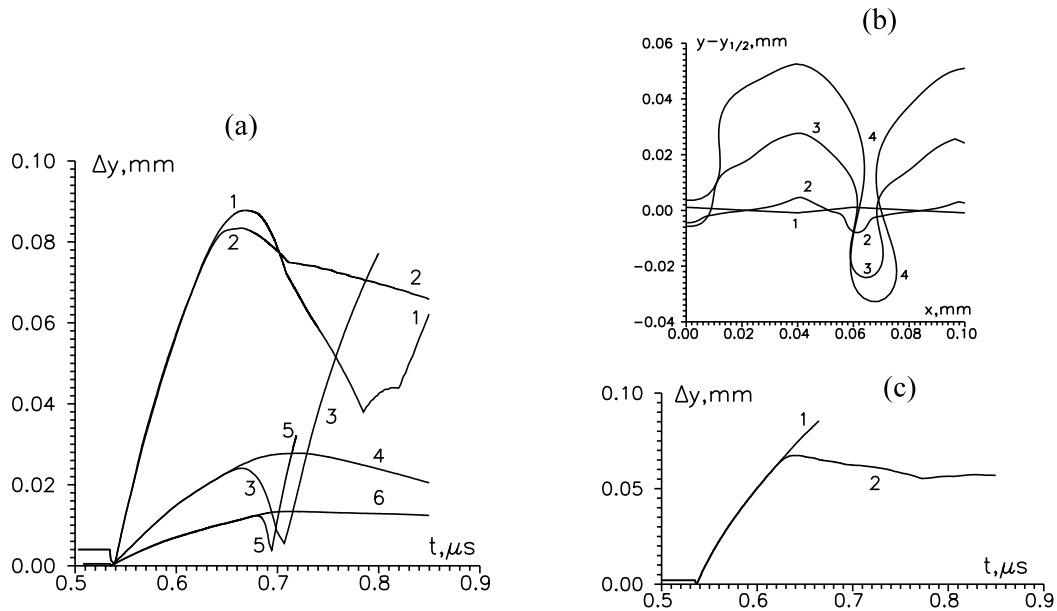


Figure 5: Reshocking. (a) Amplitude against time for sinusoidal initial perturbation: 1,2 - $\lambda = 0, 1mm$, $\beta = 5$; 3,4 - $\lambda = 0,05$, $\beta = 4$; 5,6 - $\lambda = 0,02$, $\beta = 3, 9$; 1,3,5 - a certain second shock; 2,4,6 - second shock with the aid of (1). (b) Non-sinusoidal perturbation, the free boundary at different time instants. (c) Amplitude against time for (b); 1: without second shock, 2: for the second shock with the aid of (1).

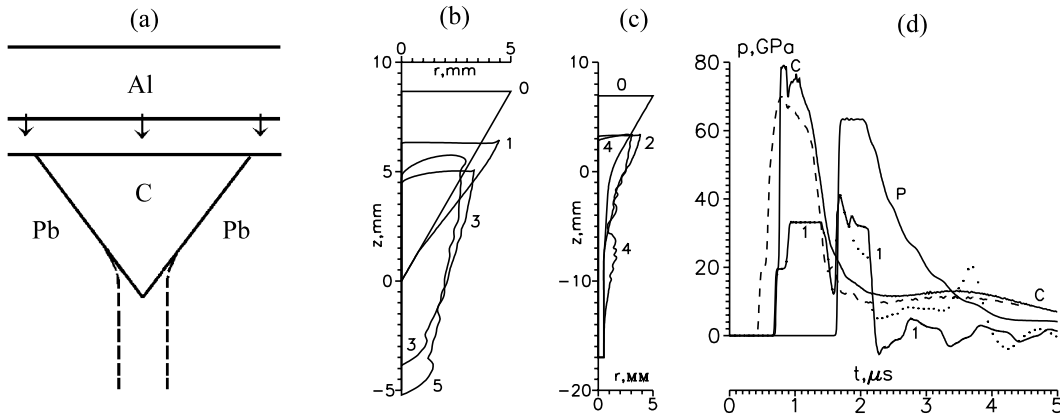


Figure 6: Graphite compression in conic targets. (a) The scheme of the problem. (b) Boundaries of the carbon volume at different time instants for the routine conic target. (c) The same for the target with the channel. (d) Pressure in a lagrangian particle on the axis of symmetry against time; 1: 1D problem with a rough model of interior destruction of the striker; points: 1D problem without the destruction taking into account; C: the conical target without the channel; dashed line: the target with the channel; P: 1D problem with lead instead of carbon.